Rapid sliding motion of a rigid frictionless indentor with a flat base over a thermoelastic half-space

G. Lykotrafitis [a] , **H.G. Georgiadis** [b,*] and **P.A. Gourgiotis** [b]

[a] *Department of Mechanical Engineering, University of Connecticut, Storrs, CT-06269, USA*

[b] *Mechanics Division, National Technical University of Athens, Zographou, GR-15773, Greece*

The paper is dedicated to Professor A.N. Kounadis on the occasion of his 75th birthday

Abstract The three-dimensional, rapid sliding indentation of a deformable half-space by a rigid indentor of a flat elliptical base is treated in this paper. The response of the material that fills the half-space is assumed to be governed by coupled thermoelasticity. The indentor translates without friction on the half-space surface at a constant sub-Rayleigh speed and the problem is treated as a steady-state one. An exact solution is obtained that is based on a Green's function approach, integral equations, and Galin's theorem. A closed-form expression for the distributed contact pressure under the elliptical base of the indentor is derived. Representative numerical results are given illustrating the effects of the indentor velocity, indentor geometry and parameters of the thermoelastic solid on the contact displacement. Since there is an analogy between the steady-state theories of thermoelasticity and poroelasticity, the present results carry over to the latter case directly.

Keywords: Contact Mechanics, Indentation, Tribology, Elastodynamics, Thermoelasticity, Three-dimensional problems, Green's function, Integral equations, Galin's theorem.

---

* Corresponding author. Tel.: +30 210 7721365; fax: +30 210 7721302.
E-mail address: *georgiad@central.ntua.gr (H.G. Georgiadis)*

1 Introduction

The indentation of a deformable half-space by a sliding rigid indentor (punch) is a key problem in Contact Mechanics and Tribology since it provides a first-step model for studies of mechanisms and surface-finishing processes.

In many cases, the problem described above can be modeled as a two-dimensional (2D) plane-strain *steady-state* situation, involving the motion of a rigid indentor that slides on the half-space at constant speed. In this context, Craggs and Roberts [1] studied the elastodynamic problem of a moving indentor and obtained physically acceptable solutions for sub-Rayleigh and supersonic sliding speeds. Subsequent work by Georgiadis and Barber [2] yielded an additional physically acceptable result for a particular speed in the transonic range and also discussed a paradox occurring in the super-Rayleigh / subseismic regime. Other efforts by Brock [3,4] dealt with the 2D sliding indentation of thermoelastic half-spaces in the presence of Coulomb friction. Later, Brock and Georgiadis [5] studied the 2D problem of sliding contact on a thermoelastic half-space at *all* speed ranges (subsonic, transonic and supersonic) of the sliding indentor. More recently, Brock and Georgiadis [6] considered the general case of *multiple* zone sliding contact involving a thermoelastic and anisotropic half-space. Their results showed the effects of sliding speed, friction and die force system on contact zone size and thermal response.

Regarding now, three-dimensional (3D) sliding contact problems (which is the topic of the present study), we notice that a rather limited number of studies exist. Churilov [7] investigated the problem of a rigid indentor with a flat elliptical base moving without friction at a constant speed on an elastic half-space. In the aforementioned work, the problem was formulated as an integral equation but no results were presented. A more detailed study was given later by Rahman [8], who examined the elastodynamic Hertz problem of a rigid indentor moving at a sub-Rayleigh speed on the surface of an elastic half-space. In this work, the unknown (elliptic) contact region was determined as part of solution from the pertinent Signorini contact conditions. More recently, Gavrilov and Herman [9] investigated the contact problem concerning the slow oscillations of a rigid frictionless circular punch, moving uniformly at a sub-Rayleigh velocity on a 3D half-space.

In closing this brief literature review, we would like to mention that related to the aforementioned sliding contact problems are some simpler problems involving the rapid motion of mechanical / thermal sources (concentrated loads / concentrated heat flux) over the surface of half-spaces. In some cases, the latter problems are the pertinent Green's functions for the more general sliding contact problems. It should also be noticed that, in general, the problems of moving sources have relevance to many situations in Contact Mechanics, Tribology and Dynamic Fracture. Typical cases are the following: (i) Motion of an asperity developed on the mating surface of mechanical systems that are pressed against each other and undergo relative sliding rapid motion accompanied by dry friction (see e.g. Ju and Huang [10], Barber [11], Kennedy [12], Huang and Ju [13]). (ii) Crack face contact in intersonic interfacial rapid fracture of bimaterial plates (Rosakis et al. [14], Huang et al. [15]). (iii) Deformations generated by the motion of high-speed modern trains (see e.g. Krylov [16], Lefeuve-Mesgouez et al. [17], Ju [18], Ju and Lin [19]). In the foregoing situations, the moving mechanical / thermal load may produce severe deformation and temperature rises in a thin zone near the contact zone, and therefore may cause excessive wear and even cracking near this zone. Representative work involving these Green's functions in 2D and 3D formulations was done by, among others, Cole and Huth [20], Georgiadis and Barber [21], Barber [22], Brock and Georgiadis [23,24], Brock and Rodgers [25], Brock et al. [26], Georgiadis and Lykotrafitis [27], and Lykotrafitis and Georgiadis [28].

The present study deals with the 3D dynamical contact problem involving the indentation of a deformable half-space by a rapidly sliding rigid body with a flat base. The indentor translates at a constant sub-Rayleigh speed and the problem is treated as a steady-state one. The case of elliptical base for the indentor treated here includes the common case of a circular base as a special one. The half-space material is taken to respond according to Biot's coupled thermoelasticity [29]. Since there is an analogy between the steady-state theories of thermoelasticity and poroelasticity (see e.g. Manolis and Beskos [30]), the present results are applicable in the latter case too. In this first-step analysis, the effect of friction is ignored and the indentor is assumed to be non-conducting. We intend to relax these assumptions in a future work. Our analysis follows closely the analyses by Churilov [7] and Rahman [8], who dealt with the non-thermal problem.

The present problem is formulated in terms of an integral equation using a Green's function approach. The pertinent Green's function, which corresponds here to the solution of the 3D steady-state problem of a point load (mechanical source) moving on the surface of a thermoelastic half-space, was derived by Lykotrafitis and Georgiadis [28]. They have developed a technique based on the Radon transform and elements of distribution theory and obtained the fundamental 3D dynamical solutions for mechanical / thermal point sources moving steadily over the surface of a thermoelastic half-space. Here, the solution of the governing integral equation (valid for the dynamical problem) is accomplished in two steps: First, the solution of the respective integral equation in the *quasi-static* case is obtained by using Galin's theorem [31], and then it is shown that this quasi-static solution satisfies also the integral equation of the dynamical problem. A closed-form expression for the distributed contact pressure under the elliptical base of the indentor is derived. Representative numerical results are given illustrating the effects of the indentor velocity and geometry on the contact displacement under a constant applied force.

2 Problem statement

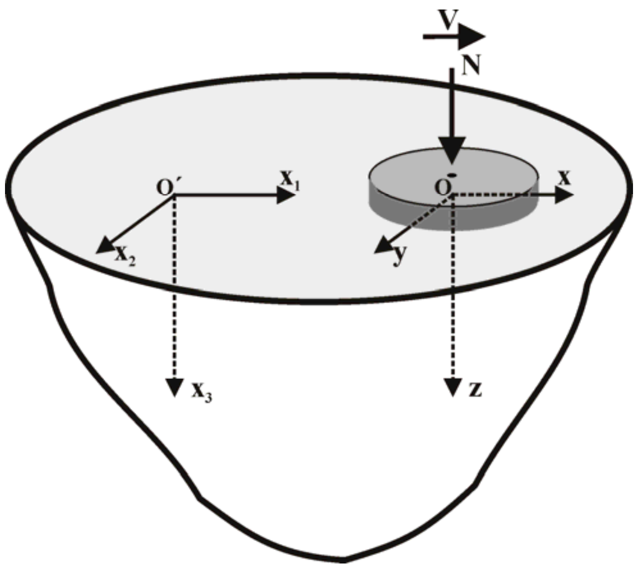

Fig. 1 Rigid indentor with a flat base moving at constant velocity over the surface of a thermoelastic half-space.

Consider a thermally conducting linearly elastic isotropic body in the form of a 3D half-space $x_3 \geq 0$. This unloaded body is initially at rest and at a uniform temperature T_0 (expressed in $^o\mathrm{K}$), but at time $t = 0$ is disturbed by the motion of a frictionless non-conducting rigid indentor (punch) of uniform flat base of elliptical form with semi-axes a and

b (see Fig. 1). The indentor moves along the x_1-direction, over the surface $x_3 = 0$, with a constant sub-Rayleigh speed V, and is pressed into contact with the half-space surface by a constant force N. The force acts at the center of the elliptical plan-form, so that the indentor does not rotate. Also, it is assumed that the surface of the elastic body outside the contact region is free from tractions and thermally insulated. Our analysis is restricted to the sub-Rayleigh regime, so as to avoid non-uniqueness of the solution or violation of the condition of non-tensile normal stress along the contact area [2].

The governing equations of the problem according to the linear coupled thermo-elastodynamic theory [29,30,32] will now be written. With respect to a fixed Cartesian coordinate system $O'x_j$ $(j=1,2,3)$, the equations of motion (thermoelastic Navier-Cauchy equations) and the generalized heat-conduction equation, in the absence of body forces and sources, along with the stress-strain relations (Duhamel-Neumann law) are as follows

$$\mu\nabla^2\mathbf{u} + (\lambda+\mu)\nabla(\nabla\cdot\mathbf{u}) - \kappa_0(3\lambda+2\mu)\nabla\theta = \rho\frac{\partial^2\mathbf{u}}{\partial t^2} \quad , \tag{1a}$$

$$K\nabla^2\theta - \rho C_v\frac{\partial\theta}{\partial t} - \kappa_0(3\lambda+2\mu)T_0\frac{\partial(\nabla\cdot\mathbf{u})}{\partial t} = 0 \ , \tag{1b}$$

$$\boldsymbol{\sigma} = \mu(\nabla\mathbf{u} + \mathbf{u}\nabla) + \lambda(\nabla\cdot\mathbf{u})\mathbf{1} - \kappa_0(3\lambda+2\mu)\theta\mathbf{1} \quad , \tag{1c}$$

where $\mathbf{u}$ is the displacement vector with components u_j, T is the current temperature, $\theta = T - T_0$ is the change in temperature, $\boldsymbol{\sigma}$ is the stress tensor with components σ_{ij} $(i,j=1,2,3)$, $\mathbf{1}$ is the identity tensor, ∇ is the 3D gradient operator, ∇^2 is the Laplace operator, $\nabla\cdot\mathbf{u}$ is the dilatation, (λ,μ) are the Lamé constants, ρ is the mass density, K is the thermal conductivity, κ_0 is the coefficient of thermal expansion, and C_v is the specific heat at constant deformation. It is also noticed that the third term in the LHS of equations (1a) and (1b) arises from the interaction of the deformation field with the thermal field. In this process, however, shear (rotational) waves remain unaffected by the ability of the medium to conduct heat; only longitudinal (dilatational) waves are modified by thermal straining and, conversely, only mechanical energy expended in volume changes is converted into heat.

We now introduce the standard *steady-state* assumption for moving sources (see e.g. [33]) according to which a steady stress and displacement field is created in the medium w.r.t.

an observer situated in a frame of reference attached to the indentor, if this indentor has been moving steadily (with a velocity V, say) for a sufficiently long time. In this way, any transients can reasonably be avoided (therefore gaining considerable simplification in the analysis) and, moreover, upon introducing the Galilean transformation

$$x = x_1 - V\,t\,, \quad y = x_2\,, \quad z = x_3 \;, \tag{2}$$

the boundary conditions become independent of the time t and the variables (x_1, t) enter the problem only in the combination $(x_1 - Vt)$. Furthermore, in the new moving Cartesian coordinate system $Oxyz$ (see Fig. 1), partial derivatives w.r.t. t are neglected and (1a), (1b) can be written as

$$\nabla^2 \mathbf{u} + (m^2 - 1)\nabla(\nabla \cdot \mathbf{u}) + \kappa \nabla \theta - m^2 c^2 \frac{\partial^2 \mathbf{u}}{\partial x^2} = 0 \;, \tag{3a}$$

$$\frac{K}{\mu}\nabla^2\theta + C_v \frac{mc}{V_T}\frac{\partial\theta}{\partial x} - \kappa T_0 c V_L \frac{\partial(\nabla\cdot\mathbf{u})}{\partial x} = 0 \;, \tag{3b}$$

where $m = (V_L/V_T) > 1$ with $V_L = [(\lambda + 2\mu)/\rho]^{1/2}$ being the longitudinal (L) wave speed in the *absence* of thermal effects and $V_T = (\mu/\rho)^{1/2}$ being the transverse (T) or shear wave speed. Also, $c \equiv M_L = V/V_L$ and $mc \equiv M_T = V/V_T$ are the two *Mach* numbers and $\kappa = \kappa_0(4 - 3m^2) < 0$. It is emphasized that V_L above is *not* the longitudinal-wave speed in coupled thermoelasticity but serves in our formulation for a convenient normalization of the field equations.

Finally, the boundary conditions of the problem take the form

$$\sigma_{zx}(x, y, z=0) = \sigma_{zy}(x, y, z=0) = 0 \qquad \text{for} \quad -\infty < x < +\infty \quad -\infty < y < +\infty \;, \tag{4a}$$

$$\partial\theta(x, y, z=0)/\partial z = 0 \qquad \text{for} \quad -\infty < x < +\infty \quad -\infty < y < +\infty \;, \tag{4b}$$

$$\sigma_{zz}(x, y, z=0) = 0 \qquad \text{for} \quad (x, y) \notin \Omega \;, \tag{4c}$$

$$u_z(x, y, z=0) = u_0 \qquad \text{for} \quad (x, y) \in \Omega \;, \tag{4d}$$

where $\Omega \equiv \left\{ \left(x, y, z = 0 \right) : \left(x^2/a^2 + y^2/b^2 \leq 1 \right) \right\}$ is the contact area, and u_0 is the (constant) contact displacement. The main objective of the present work is to determine the contact pressure $\sigma_{zz}\left(x, y, z = 0 \right) \equiv -p\left(x, y \right)$ that is produced by the force N (exerted on the indentor) for the problem described by Eqs. (1c), (3) and (4).

3 The thermo-elastodynamic Green's function

The solution of the mixed boundary problem described in the previous Section will be obtained using a Green's function approach. The pertinent Green's function, which here corresponds to the problem of a concentrated normal load P moving steadily along the x_1-direction with a constant velocity V over the surface of a thermoelastic half-space (Fig. 2), was derived by Lykotrafitis and Georgiadis [28]. In the latter study, the fundamental thermoelastic three-dimensional solutions for moving thermal and/or mechanical point sources were obtained employing a technique based on the Radon transform and distribution theory.

In this Section, we essentially reproduce relevant material from the work by Lykotrafitis and Georgiadis [28]. This material is briefly presented here for the sake of completeness and because of the need to introduce certain definitions.

The boundary conditions of the problem take the form (see Fig. 2)

$$\sigma_{zz}\left(x,y,z=0 \right) = -P \cdot \delta\left(x \right) \cdot \delta\left(y \right) \quad , \tag{5a}$$

$$\sigma_{zx}\left(x, y, z = 0 \right) = 0 \quad , \tag{5b}$$

$$\sigma_{zy}\left(x , y , z = 0 \right) = 0 \quad , \tag{5c}$$

$$\frac{\partial \theta\left(x, y, z = 0 \right)}{\partial z} = 0 \quad , \tag{5d}$$

which hold for $-\infty < x < +\infty$ and $-\infty < y < +\infty$. In the above equations, $\delta()$ is the Dirac delta distribution.

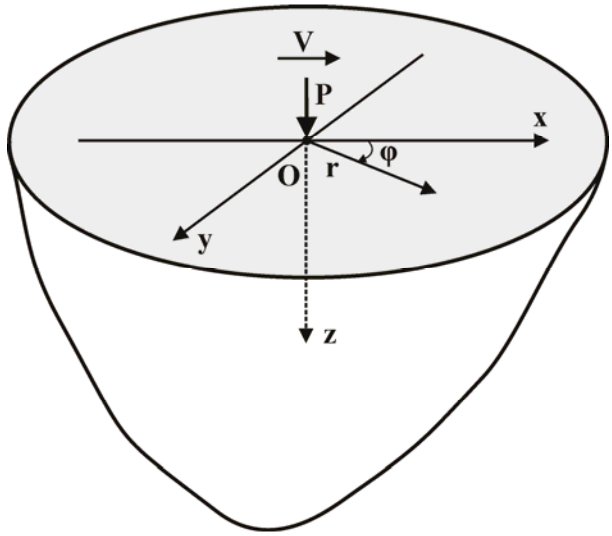

Fig. 2 Normal point load moving at constant velocity over the surface of a half-space.

The solution of the boundary value problem is effected through a technique based on the Radon transform [34] and pertinent coordinate transformations. In general, this procedure reduces the original 3D problem to a pair of auxiliary problems, i.e. a corresponding 2D plane-strain problem and a 2D anti-plane shear problem. However, in our case where only a concentrated *normal* load is involved, the 3D problem reduces to a *pure* 2D plane-strain problem. In fact, this 2D plane-strain problem is completely analogous to the original 3D problem, not only regarding the field equations but also regarding the boundary conditions.

The 2D Radon transform of a function $f(\mathbf{r})$, with $|\mathbf{r}| = (x^2 + y^2)^{1/2}$, is defined as

$$\Re(f(\mathbf{r})) \equiv \tilde{f}(q,\omega) = \iint f(\mathbf{r}) \cdot \delta(q - \mathbf{n} \cdot \mathbf{r}) d\mathbf{r} = \int_L f(x,y) ds \ , \tag{6}$$

where L denotes all straight lines in the plane Oxy and ds is the infinitesimal length along such a line. The lines L are defined by $\mathbf{n} \cdot \mathbf{r} = q$, with $\mathbf{n} \equiv (n_x, n_y) = (\cos\omega, \sin\omega)$, and the Radon transform is in fact the integral of $f(\mathbf{r})$ over all these straight lines in the plane. The inverse 2D Radon transform is given by

$$f(x,y)=f(r,\varphi)=-\frac{1}{4\pi^2}\int_0^{2\pi}\left(\left(\int_{-\infty}^{+\infty}\frac{\partial\tilde{f}(q,\omega)}{\partial q}\cdot\mathbf{PF}\left(\frac{1}{q-r\cdot\cos(\omega-\varphi)}\right)dq\right)d\omega\right) \quad , \qquad (7)$$

where the symbol $\mathbf{PF}(\;)$ stands for the *principal-value* pseudo-function (or distribution) (see e.g. [34-36]).

Next, operating with the Radon transform on the governing equations (3), using standard properties of the Radon transform (linearity, and transforms of derivatives and distributions) and performing a rotation of the original (x,y,z) coordinate system through the angle ω about the z-axis, gives the following field equations in the new coordinate system

$$\frac{\partial^2\tilde{u}_q}{\partial q^2}+\frac{\partial^2\tilde{u}_q}{\partial z^2}+(m^2-1)\frac{\partial}{\partial q}\left(\frac{\partial\tilde{u}_q}{\partial q}+\frac{\partial\tilde{u}_z}{\partial z}\right)+\kappa\frac{\partial\tilde{\theta}}{\partial q}-m^2c_x^2\frac{\partial^2\tilde{u}_q}{\partial q^2}=0 \qquad (8a)$$

$$\frac{\partial^2\tilde{u}_z}{\partial q^2}+\frac{\partial^2\tilde{u}_z}{\partial z^2}+(m^2-1)\frac{\partial}{\partial z}\left(\frac{\partial\tilde{u}_q}{\partial q}+\frac{\partial\tilde{u}_z}{\partial z}\right)+\kappa\frac{\partial\tilde{\theta}}{\partial z}-m^2c_x^2\frac{\partial^2\tilde{u}_z}{\partial q^2}=0 \quad , \qquad (8b)$$

$$\frac{K}{\mu}\left(\frac{\partial^2\tilde{\theta}}{\partial q^2}+\frac{\partial^2\tilde{\theta}}{\partial z^2}\right)+C_v\frac{mc_x}{V_T}\frac{\partial\tilde{\theta}}{\partial q}-\kappa T_0c_xV_L\frac{\partial}{\partial q}\left(\frac{\partial\tilde{u}_q}{\partial q}+\frac{\partial\tilde{u}_z}{\partial z}\right)=0 \quad , \qquad (8c)$$

whereas the transformed boundary conditions become

$$\tilde{\sigma}_{zz}(q,\omega,z=0)=-P\cdot\delta(q), \qquad (9a)$$

$$\tilde{\sigma}_{zq}(q,\omega,z=0)=0, \qquad (9b)$$

$$\frac{\partial\tilde{\theta}(q,\omega,z=0)}{\partial z}=0, \qquad (9c)$$

where $c_x\equiv cn_x$.

One may observe that Eqs. (8) and (9) form a 2D *plane-strain* problem in the (q,z) coordinate system. This problem involves a thermoelastic body in the form of the half-plane $z\geq 0$ that is disturbed by the steady-state motion of a concentrated normal line load P, which moves along the q-axis with velocity $V_q\equiv V\cdot\cos\omega$. The solution to this 2D problem has been obtained by Brock and Georgiadis [23] through the two-sided Laplace transform and exact inversions.

Then, the 3D solution follows from the transformed solution in two steps. First, the inversion of the coordinate transformation is performed providing the set $\left(\tilde{u}_z, \tilde{u}_x, \tilde{u}_y\right)$ in terms of the rotated Radon-transformed displacements $\left(\tilde{u}_z, \tilde{u}_q\right)$. Then, the Radon-transform inversion according to Eq. (7) gives the set $\left(u_z, u_x, u_y\right)$ in the physical domain. Indeed, operating with Eq. (7) on the solution of the plane strain problem and using results from distribution theory along with results concerning the Hilbert transform of generalized functions [36], we obtain the surface vertical displacement as

$$u_z^{(P)}\left(r,\varphi,z=0\right) = -\frac{P}{\mu r}\left\{\frac{1}{2}F_1^{(P)}\left(M_T\sin\varphi,\varepsilon\right) + \right.$$
$$\left. + \frac{\cos\varphi}{\pi^2}\left[\left[\int_0^1 F_2^{(P)}\left(M_T\left(1-\zeta^2\right)^{1/2},\varepsilon\right)\cdot \mathbf{PF}\left(\frac{1}{\cos^2\varphi-\zeta^2}\right)d\zeta\right]\right]\right\} \quad , \tag{10}$$

where the functions $F_1^{(P)}(\ )$ and $F_2^{(P)}(\ )$ are given in [28] for the *entire* speed range. In particular, in the sub-Rayleigh regime ($0 < V < V_{R\varepsilon}$), which is the case of interest here, the functions are as follows

$$F_1^{(P)}\left(M_T,\varepsilon\right) = \frac{M_T^2\left(1-M_{L\varepsilon}^2\right)^{1/2}}{\pi R_\varepsilon\left(M_T,\varepsilon\right)} \quad , \qquad F_2^{(P)}\left(M_T,\varepsilon\right) = 0 \ . \tag{11a,b}$$

These functions depend upon the 'shear' (or 'transverse') Mach number M_T and the dimensionless coupling constant $\varepsilon \equiv \left(T_0/C_v\right)\left(\kappa V_T/m\right)^2$. The order of magnitude of the coupling constant for usual metallic materials (e.g. aluminum, copper, lead, titanium and steel) is $\varepsilon = O\left(10^{-2}\right)$, but in other cases ε can be as high as $O\left(10^{-1}\right)$ (e.g. $\varepsilon = 0.36$ for polycarbonate at $T_0 = 40^o C$). Moreover, in Eq. (11) the following definitions are employed. First, it is noticed that the quantity $V_{L\varepsilon} = V_L\left(1+\varepsilon\right)^{1/2}$ represents the *steady-state* velocity of thermoelastic longitudinal waves [23], whereas $M_{L\varepsilon} \equiv V/V_{L\varepsilon} = M_L/\left(1+\varepsilon\right)^{1/2}$ is the 'thermoelastic longitudinal' Mach number. Then, the *steady-state* thermoelastic Rayleigh function defined as [23]

$$R_{\varepsilon}\left(M_T,\varepsilon\right)=\left(2-M_T^2\right)^2-4\left(1-M_{L\varepsilon}^2\right)^{1/2}\left(1-M_T^2\right)^{1/2} \quad , \tag{12}$$

provides the steady-state thermoelastic Rayleigh-wave speed $V_{R\varepsilon}$ as the non-trivial *real* root $m_{1\varepsilon}$ of the equation $R_{\varepsilon}\left(M_T,\varepsilon\right)=0$. By following the standard procedure for the rationalization of the Rayleigh equation into a cubic in square of speed (see e.g. Sokolnikoff [37], and Rahman and Barber [38]), the root $m_{1\varepsilon}\equiv V_{R\varepsilon}/V_T$ is obtained with the aid of MATHEMATICA™ (see Appendix A). We should also mention that an alternative procedure to obtain the Rayleigh-wave speed is performing a factorization operation typically encountered in the Wiener-Hopf technique (Brock [39]). It is also noticed that the Mach numbers $M_{L\varepsilon}$ and M_T are related, by their definition, through the following equation

$$M_{L\varepsilon}=\frac{1}{m_{\varepsilon}}M_T \quad , \qquad \text{with} \qquad m_{\varepsilon}\equiv\frac{V_{L\varepsilon}}{V_T}=\left(\frac{2\left(1-\nu\right)\left(1+\varepsilon\right)}{\left(1-2\nu\right)}\right)^{1/2}>1 \quad , \tag{13}$$

where ν is the Poisson's ratio of the material.

In light of the above, the surface vertical displacement in (10) takes now the form

$$u_z^{(P)}\left(r,\varphi,z=0\right)=-\frac{P}{2\mu\, r}F_1^{(P)}\left(M_T\sin\varphi,\varepsilon\right) \; , \qquad 0<V<V_{R\varepsilon} \; . \tag{14}$$

Equation (14) is the pertinent Green's function for our thermo-elastodynamic contact problem. One may observe that (14) implies the symmetry of $u_z^{(P)}$ w.r.t. both axes x and y.

For illustration, in Fig. 3 the variation of the normalized displacement $U_z^{(P)}$ is displayed with respect to the polar angle φ for a material with Poisson's ratio $\nu=0.3$ and two different thermoelastic coupling constants $\varepsilon=0$ and $\varepsilon=0.36$. It is observed that in the sub-Rayleigh range (M_T =0.8) the displacement is always positive and, therefore, is directed into the half-space.

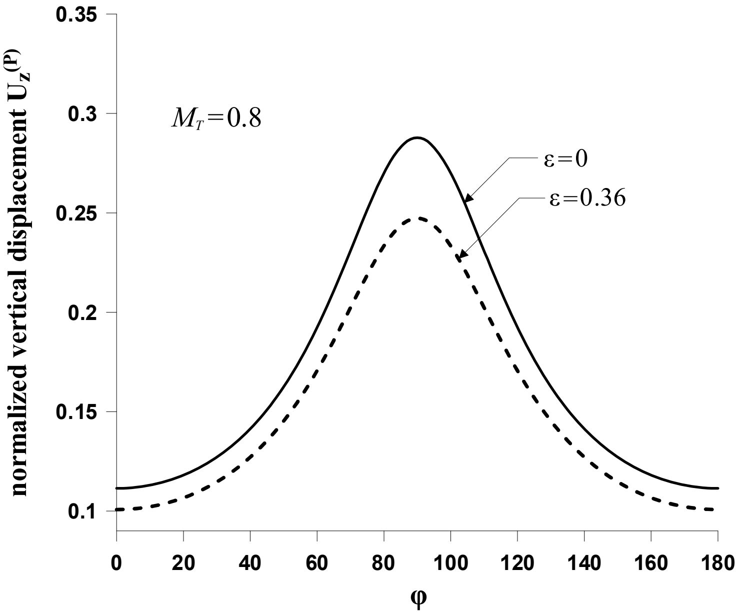

Fig. 3. Variation of the normalized vertical displacement $U_z^{(P)} = u_z^{(P)} \mu r / P$, due to a normal moving load P, with the polar angle φ for sub-Rayleigh motion and for $M_T = 0.8$ and $\nu = 0.3$.

4 Integral equation solution

The deformation of the surface caused by the normal compressive stresses distributed over the contact region Ω can be found by superposition, using (14) as the Green's function for the contact problem. Indeed, treating the distributed pressure as the limit of a set of point loads of magnitude $p(\xi,\eta)\, d\xi\, d\eta$, the normal surface displacement takes the following form

$$u_z(x,y,0) = -\frac{1}{2\mu} \iint_{\Omega} \frac{p(\xi,\eta)}{s} \cdot F_1^{(P)}\left(M_T \frac{(y-\eta)}{s}, \varepsilon \right) d\xi\, d\eta \ , \tag{15}$$

where $s = \left[(x-\xi)^2 + (y-\eta)^2 \right]^{1/2}$ is the distance between the points (x,y) and (ξ,η) as Fig. 4 shows.

Next, employing Eq. (15) in conjunction with the boundary condition in (4d), we derive an integral equation of the first kind for the unknown pressure $p(\xi,\eta)$

$$u_0 = -\frac{1}{2\mu}\iint_{\Omega} \frac{p(\xi,\eta)}{s} \cdot F_1^{(P)}\left(M_T \frac{(y-\eta)}{s}, \varepsilon \right) d\xi \, d\eta \ , \quad \text{for} \quad (x,y) \in \Omega \ . \tag{16}$$

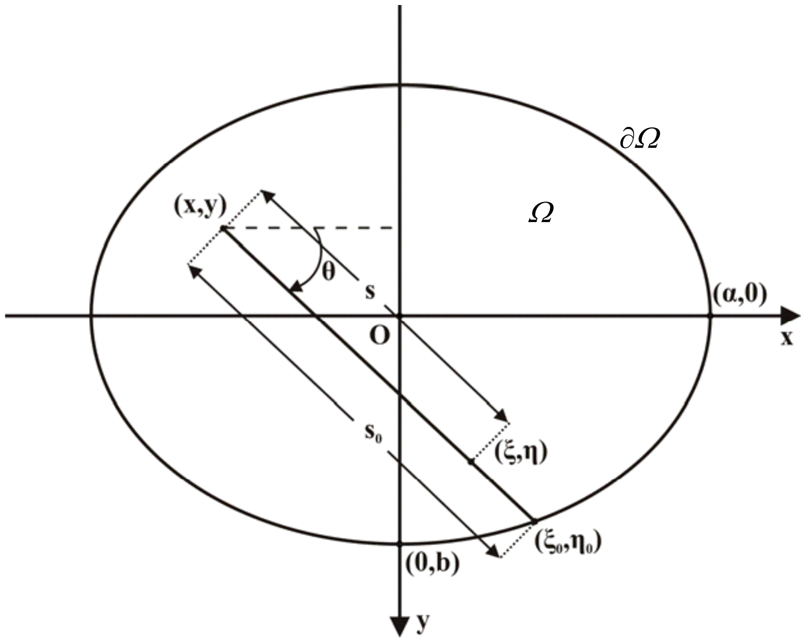

Fig. 4 Elliptical contact region Ω with semi-axes a and b .

The solution of the above integral equation will be accomplished in two steps. First, the solution of the respective integral equation in the *quasi-static* case will be obtained, and then it will be shown that this solution satisfies also the 'thermo-elastodynamic' integral equation (16).

By letting $V \to 0$, the integral equation in (16) degenerates into its elastostatic counterpart

$$u_0 = -\frac{1}{2\mu}\iint_{\Omega} \frac{p(\xi,\eta)}{s} \cdot F_1^{(P)}(0,\varepsilon) \, d\xi \, d\eta \ , \tag{17}$$

where the function $F_1^{(P)}(0,\varepsilon)$ is given by (see Appendix A)

$$F_1^{(P)}\left(0,\varepsilon\right)=-\frac{\left(1-\nu\right)\left(1+\varepsilon\right)}{\pi\left[1+2\varepsilon\left(1-\nu\right)\right]} \ . \tag{18}$$

Then, in view of (18), Eq. (17) becomes

$$u_0=\frac{\left(1-\nu\right)\left(1+\varepsilon\right)}{2\mu\pi\left[1+2\varepsilon\left(1-\nu\right)\right]}\iint_{\Omega}\frac{p\left(\xi,\eta\right)}{s}d\xi\, d\eta \ . \tag{19}$$

A solution of this type of integral equation, when Ω is an elliptical region, can be obtained by using Galin's theorem [31]. As was pointed out by Walpole [40], this theorem is a special case of a more general result due to Dyson [41]. A comprehensive account of Galin's theorem and its generalizations can be found in the treatise by Gladwell [42]. In fact, Galin's theorem states that if the equation of the surface bounding the base of the indentor is of the form $u_z\left(x,y,0\right)=h_n\left(x,y\right)$, where $h_n\left(x,y\right)$ is a polynomial of degree n, then the solution for the pressure under the punch can be represented in the following form

$$p\left(x,y\right)=\left(1-\frac{x^2}{a^2}-\frac{y^2}{b^2}\right)^{-1/2}h_n^*\left(x,y\right) \ , \tag{20}$$

where $h_n^*\left(x,y\right)$ is also a polynomial of degree n.

Now, in the special case of a punch with a *flat* elliptical base ($n=0$), Galin's theorem provides the following solution for the quasi-static integral equation (19)

$$p\left(\xi,\eta\right)=\frac{p_0}{\left(1-\xi^2/a^2-\eta^2/b^2\right)^{1/2}} \ , \tag{21}$$

where the constant p_0 can be obtained directly by elementary considerations of equilibrium. Indeed, since the pressure distribution is statically equivalent to the force N, which is exerted on the contact area, we can write

$$N = \iint_{\Omega} p(\xi,\eta)\, d\xi d\eta = p_0 \iint_{\Omega} \left(1 - \frac{\xi^2}{a^2} - \frac{\eta^2}{b^2}\right)^{-1/2} d\xi d\eta = p_0 (2\pi ab) \ . \tag{22}$$

It remains now to prove that the solution (21) satisfies also the integral equation (16) for the thermo-elastodynamic case considered here. In doing so, we closely follow the approach proposed by Vorovich et al. [43] and Rahman [8] for the pure elastodynamic case. The following analysis is somewhat tedious but straightforward.

First, one has to introduce a new set of polar coordinates (s,θ) attached to the field point (x,y) and defined through the relations (see Fig. 4):

$$\xi = x + s\cos\theta \ , \tag{23a}$$

$$\eta = y + s\sin\theta \ . \tag{23b}$$

Further, substituting from (23) into Eq. (21) yields

$$p(\xi,\eta) = p(x + s\cos\theta,\ y + s\sin\theta) = p_0 \left[A - 2B(\theta)s - C(\theta)s^2\right]^{-1/2} \ , \tag{24}$$

where

$$A = 1 - x^2/a^2 - y^2/b^2 \ , \tag{25a}$$

$$B = x\cos\theta/a^2 + y\sin\theta/b^2 \ , \tag{25b}$$

$$C = \cos^2\theta/a^2 + \sin^2\theta/b^2 \ , \tag{25c}$$

with $B(\theta+\pi) = -B(\theta)$ and $C(\theta+\pi) = C(\theta)$.

Next, substituting (24) and (25) in the integral equation (16), and by invoking (23) and the fact that $F_1^{(P)}(M_T,\varepsilon)$ is an even function of M_T, we obtain

$$u_0 = -\frac{p_0}{2\mu}\int_0^{2\pi}\int_0^{s_0(\theta)} \left[A - 2B(\theta)s - C(\theta)s^2\right]^{-1/2} \cdot F_1^{(P)}(M_T \sin\theta,\varepsilon)\ ds\, d\theta \ , \tag{26}$$

where $s_0(\theta)$ is the distance between the points (x, y) and (ξ_0, η_0), with $(\xi_0, \eta_0) \in \partial\Omega$ (see Fig. 4). In addition, since the point (ξ_0, η_0) lies on the boundary of the ellipse, the following equations hold true

$$\xi_0^2 / a^2 + \eta_0^2 / b^2 = 1 \ , \tag{27}$$

$$\xi_0 = x + s_0 \cos\theta \ , \tag{28a}$$

$$\eta_0 = y + s_0 \sin\theta \ . \tag{28b}$$

Employing now Eqs. (25) in conjunction with (28), we may write (27) as

$$\frac{C(\theta)}{2} s_0^2 + B(\theta) s_0 - \frac{A}{2} = 0 \ , \tag{29}$$

which admits the following solution since $s_0(\theta) \geq 0$ must hold for all $\theta \in [0, 2\pi]$

$$s_0(\theta) = \frac{-B(\theta) + \left[B^2(\theta) + AC(\theta)\right]^{1/2}}{C(\theta)} \ . \tag{30}$$

On the other hand, since the point (x, y) lies in the interior of the ellipse, it can be deduced from (25a,c) that $A > 0$ and $C(\theta) > 0$ for all $\theta \in [0, 2\pi]$. Thus,

$$\frac{B}{\left(B^2 + AC\right)^{1/2}} \leq \frac{B + sC}{\left(B^2 + AC\right)^{1/2}} \leq \frac{B + s_0 C}{\left(B^2 + AC\right)^{1/2}} \ . \tag{31}$$

Also, from (25) and (30), we infer that

$$B + \left(B^2 + A\,C\right)^{1/2} \geq 0 \Leftrightarrow \frac{B}{\left(B^2 + A\,C\right)^{1/2}} \geq -1 \ , \tag{32}$$

and

$$\frac{B+s_0\ C}{\left(B^2+A\ C\right)^{1/2}}=1\ . \tag{33}$$

Finally, by combining Eqs. (31)-(33), one may confirm that

$$-1\leq\frac{B+s\ C}{\left(B^2+A\ C\right)^{1/2}}\leq1\ . \tag{34}$$

Now, in view of (34), we introduce a new variable ω through the relation

$$\cos\omega=\frac{B+s\ C}{\left(B^2+A\ C\right)^{1/2}}\qquad\text{with }\ 0\leq\omega\leq\pi\ , \tag{35}$$

which, in turn, implies that

$$ds=-\frac{1}{C(\theta)^{1/2}}\left[A-2B(\theta)s-C(\theta)s^2\right]^{1/2}d\omega\ . \tag{36}$$

In light of the above, Eq. (26) becomes

$$u_0=-\frac{p_0}{2\mu}\int_0^{2\pi}\int_0^{\omega(\theta)}F_1^{(P)}\left(M_T\sin\theta,\varepsilon\right)\cdot C(\theta)^{-1/2}\,d\omega\,d\theta\ \ , \tag{37}$$

where $\omega(\theta)=\arccos\left[B(\theta)\Big/\left[B^2(\theta)+AC(\theta)\right]^{1/2}\right]$ is the new integration limit that corresponds to $s=0$ in Eq. (35).

At this point, we consider the integral

$$I=\int_\pi^{2\pi}\int_0^{\omega(\theta)}F_1^{(P)}\left(M_T\sin\theta,\varepsilon\right)\cdot C(\theta)^{-1/2}\,d\omega\,d\theta\ . \tag{38}$$

Further, we change the integration variable to $\theta = \psi + \pi$, and note that $\cos\omega(\psi+\pi) = -\cos\omega(\psi)$ when $s = 0$. Thus, since $0 \le \omega \le \pi$, it follows also that $\omega(\psi+\pi) = \pi - \omega(\psi)$. In view now of the previous observations and invoking the properties of the function $C(\theta)$, we obtain

$$I = \int_0^{\pi} \int_0^{\pi-\omega(\psi)} F_1^{(P)}\left(-M_T \sin\psi, \varepsilon\right) \cdot C(\psi)^{-1/2} \, d\omega \, d\psi \ . \tag{39}$$

Moreover, putting $\omega = \pi - \omega'$ into (39) and taking again into account that $F_1^{(P)}\left(M_T, \varepsilon\right)$ is an even function of M_T, we get

$$I = \int_0^{\pi} \int_{\omega(\psi)}^{\pi} F_1^{(P)}\left(M_T \sin\psi, \varepsilon\right) \cdot C(\psi)^{-1/2} \, d\omega' \, d\psi \ , \tag{40a}$$

or equivalently

$$I = \int_0^{\pi} \int_{\omega(\theta)}^{\pi} F_1^{(P)}\left(M_T \sin\theta, \varepsilon\right) \cdot C(\theta)^{-1/2} \, d\omega \, d\theta \, . \tag{40b}$$

Finally, with the aid of (38) and (40b), the integral equation in (37) reduces to

$$u_0 = -\frac{p_0}{2\mu} \int_0^{\pi} F_1^{(P)}\left(M_T \sin\theta, \varepsilon\right) \cdot C(\theta)^{-1/2} \, d\theta \cdot \left\{ \int_0^{\pi} d\omega \right\} \ , \tag{41}$$

which, after integrating with respect to ω, yields

$$u_0 = -\frac{p_0 \pi}{2\mu} \int_0^{\pi} F_1^{(P)}\left(M_T \sin\theta, \varepsilon\right) \cdot C(\theta)^{-1/2} \, d\theta \ . \tag{42}$$

Now, in view of (11) and (25c), the RHS of Eq. (42) is clearly independent of the variables (x, y) and this shows that the quasi-static solution in (21) describes the traction distribution in the contact area of the thermo-elastodynamic problem, as well. However, it should be emphasized that this is the case *only* when the indentor moves with a sub-Rayleigh speed. Indeed, in the super-Rayleigh regime the pertinent Green's function is *not* an even function of the shear Mach number M_T [28] and, therefore, the above procedure cannot be applied. In fact, in that case, the quasi-static solution (21) would not eliminate the dependence on the spatial variables (x, y) in the RHS of the pertinent thermo-elastodynamic integral equation in (16).

5 Numerical results

Based on the previous analysis, we are now able to evaluate the displacement u_0 along the contact area in terms of the applied normal force N and the velocity V of the indentor. Indeed, by virtue of Eqs. (21), (22) and (42), u_0 can be written as

$$u(x, y, z=0) = u_0 = -\frac{N}{4\mu ab} \int_0^{\pi} F_1^{(P)}(M_T \sin\theta, \varepsilon) \cdot C(\theta)^{-1/2} d\theta \quad \text{for } (x, y) \in \Omega \ , \quad (43)$$

whereas the pressure along the contact area is given by

$$\sigma_{zz}(x, y, z=0) \equiv -p(x, y) = -\frac{N}{2\pi ab} \frac{1}{\left(1 - x^2/a^2 - y^2/b^2\right)^{1/2}} \quad \text{for } (x, y) \in \Omega \ . \quad (44)$$

It is noted that the normal stress in (44) exhibits a square root singularity at the edge $(x, y) \in \partial\Omega$ of the contact region. Moreover, as $V \to 0$, Eq. (43) in conjunction with (18) provides the displacement along the contact area of the counterpart quasi-static problem

$$u_0^{stat.} = \frac{N}{4\mu\pi ab} \frac{(1-v)(1+\varepsilon)}{1+2\varepsilon(1-v)} \int_0^{\pi} C(\theta)^{-1/2} d\theta \quad \text{for } (x, y) \in \Omega \text{ and } z = 0 \ . \quad (45)$$

Now, in view of (25c), the integral in (45) can be evaluated in closed form yielding the following expression

$$u_0^{stat.} = \frac{N}{2\mu\pi a} \frac{(1-\nu)(1+\varepsilon)}{1+2\varepsilon(1-\nu)} K\left[\left(1-(b/a)^2\right)^{1/2}\right] \quad \text{for } (x,y)\in\Omega \text{ and } z=0 , \qquad (46)$$

where $K[\ ]$ is the complete Elliptic integral of the first kind [44]. It is noted that by setting $\varepsilon = 0$ in (46), we obtain the respective result for the pure elastostatic case [45].

Some numerical results are presented now showing the variation of the normalized contact displacement $U_0 \equiv 4\mu a u_0 / N$ as a function of the shear Mach number M_T (normalized punch velocity).

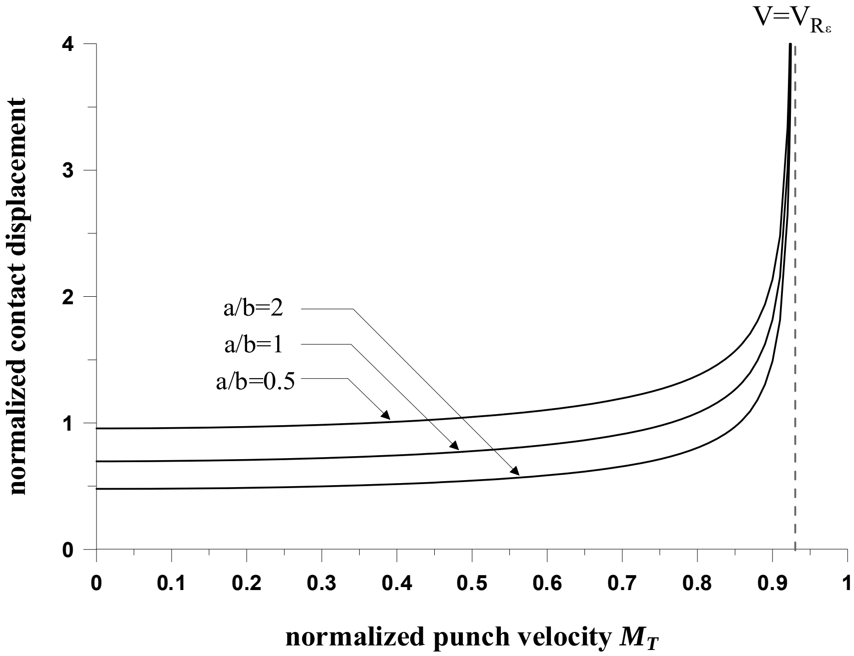

Fig. 5 Variation of the normalized contact displacement U_0 with respect to the normalized punch velocity M_T for three different ratios a/b .

Figure 5 depicts the variation of U_0 with the shear Mach number M_T for a material with Poisson's ratio $\nu = 0.3$ and thermoelastic coupling constant $\varepsilon = 0.011$. Three different ratios of semi-axes a/b are considered for the elliptical base of the punch. It is observed that for $0 < V < V_{R\varepsilon}$ the contact displacement is always greater than its static counterpart displacement $u_0^{stat.}$ (the latter is given by Eq. (46)). On the other hand, as the punch velocity V approaches the Rayleigh wave velocity ($V_{R\varepsilon}/V_T = 0.927$), the contact displacement becomes infinite, no matter how small the intensity of the force N is. Therefore, in light of the above, one may observe that below the Rayleigh wave speed the present thermo-elastodynamic solution behaves as the static indentation of a half-space with a *reduced* modulus. This 'modulus' approaches zero as $V \to V_{R\varepsilon}$. Of course, the latter result can be of practical importance in certain manufacturing processes.

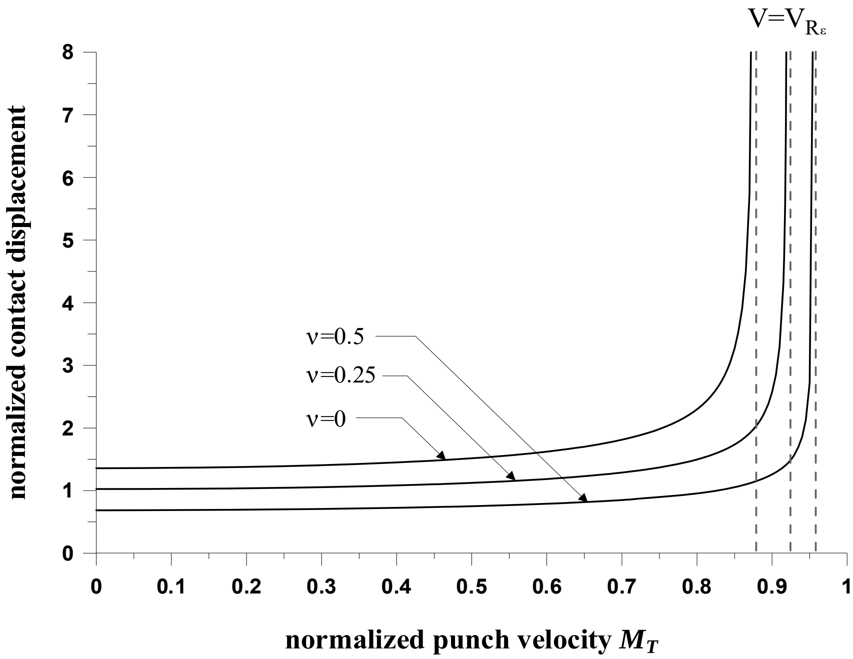

Fig. 6 Variation of the normalized contact displacement U_0 with the normalized punch velocity M_T for different values of the Poisson's ratio ν.

Figure 6, now, displays the dependence of the contact displacement U_0 upon the Poisson's ratio, for a punch with an elliptical base with ratio of semi-axes $a/b = 2$. The coupling constant is $\varepsilon = 0.011$. The lowest Rayleigh wave velocity in this case is given by $V_{R\varepsilon}/V_T = 0.876$ for the case $\nu = 0$. As anticipated on intuitive grounds, the contact displacement decreases with increasing values of the Poisson's ratio. For example, when the normalized indentor velocity is $M_T = 0.85$, a 67% decrease is noted in the contact displacement for an incompressible material ($\nu = 0.5$) as compared to a material with Poisson's ratio $\nu = 0$.

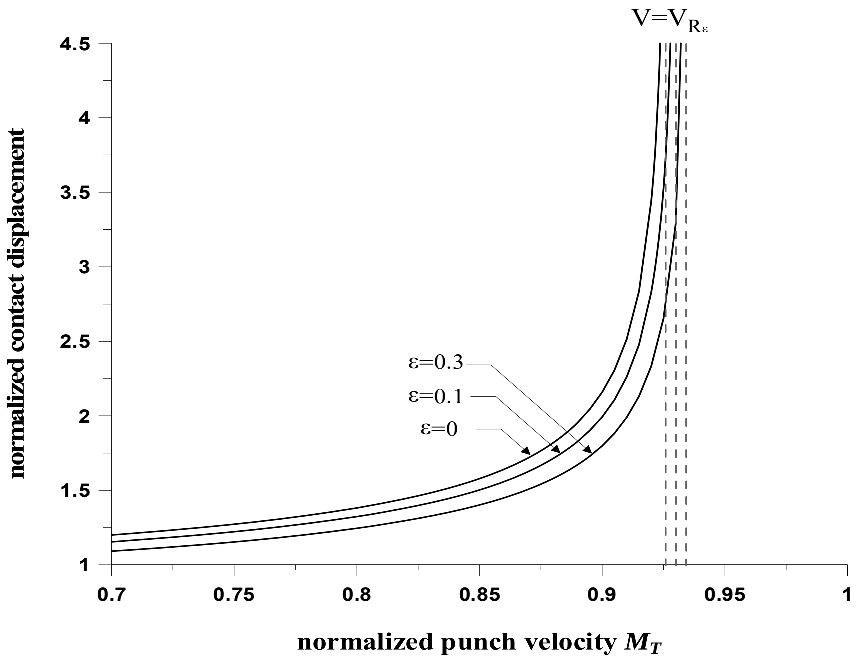

Fig. 7 Variation of the normalized contact displacement U_0 with the normalized punch velocity M_T for different values of the thermoelastic coupling constant ε.

Finally, Fig. 7 shows the influence of thermal effects on the contact displacement U_0, for an indentor with an elliptical base with ratio of semi-axes $a/b = 2$ and a half-space material of Poisson's ratio $\nu = 0.3$. The lowest Rayleigh wave velocity ($V_{R\varepsilon}/V_T = 0.927$) corresponds to the case $\varepsilon = 0$ (no thermal effects). It is observed that a decrease in the contact displacement takes place when thermal effects are taken into account. This decrease becomes quite significant when the velocity of the indentor becomes comparable to the pertinent Rayleigh wave velocity.

Concluding remarks

The 3D steady-state thermo-elastodynamic contact problem of a rigid indentor that slides over the surface of a half-space is treated, for the first time, in this paper. It is assumed that the punch has a flat base and it is thermally non-conducting. Also, the punch moves rectilinearly at a constant sub-Rayleigh speed and without friction. The half-space material responds according to Biot's thermoelasticity. An exact solution is obtained through integral equations by using a Green's function approach. In the absence of thermal effects, the present formulation reduces to the 3D elastodynamic case considered by Rahman [8]. Our results illustrate the effects of the indentor velocity, indentor geometry and parameters of the thermoelastic solid on the contact displacement. These effects are greatly pronounced when the punch velocity approaches the thermoelastic Rayleigh wave speed. Because of the mathematical analogy between the steady-state theories of thermoelasticity and poroelasticity, the present results carry over to the latter case directly. We intend to relax the assumption of frictionless sliding in a study that is underway.

Acknowledgement

The authors acknowledge with thanks support from the 'ΠΕΒΕ 2010' programme of NTU Athens (# 65/1843, title of the individual project: 'Dynamic Fracture and Contact within the Framework of Generalized Continua and Thermo-Mechanics').

Appendix A

First, we multiply the thermoelastic function $R_\varepsilon\left(M_T,\varepsilon\right)$ in (12) with the expression $\left(2-M_T^2\right)^2+4\left(1-M_{L\varepsilon}^2\right)^{1/2}\left(1-M_T^2\right)^{1/2}$ and obtain

$$K_\varepsilon\left(M_T,\varepsilon\right)=M_T^2\left[M_T^6-8M_T^4+8\left(3-2m_\varepsilon^{-2}\right)M_T^2-16\left(1-m_\varepsilon^{-2}\right)\right]=$$
$$=M_T^2\left(M_T^2-m_{1\varepsilon}\right)\left(M_T^2-m_{2\varepsilon}\right)\left(M_T^2-m_{3\varepsilon}\right)\quad, \qquad \text{(A.1)}$$

where $(m_{1\varepsilon}, m_{2\varepsilon}, m_{3\varepsilon})$ are the non-trivial zeros of $K_\varepsilon(M_T, \varepsilon)$ and $m_\varepsilon = \left[2(1-\nu)(1+\varepsilon)/(1-2\nu)\right]^{1/2}$. Next, we use MATHEMATICA$^{\mathrm{TM}}$ obtaining the following expressions for these zeros

$$m_{1\varepsilon} = \frac{4}{3}\left[2 + \frac{2^{1/3}(5\nu_\varepsilon - 2)}{\beta(\nu_\varepsilon)} - \frac{2^{2/3}}{4(1-\nu_\varepsilon)}\beta(\nu_\varepsilon)\right], \qquad \text{(A.2a)}$$

$$m_{2\varepsilon} = \frac{2}{3}\left[4 - \frac{2^{1/3}(1-\mathrm{i}3^{1/2})(5\nu_\varepsilon - 2)}{\beta(\nu_\varepsilon)} + \frac{2^{2/3}(1+\mathrm{i}3^{1/2})}{4(1-\nu_\varepsilon)}\beta(\nu_\varepsilon)\right], \qquad \text{(A.2b)}$$

$$m_{3\varepsilon} = \frac{2}{3}\left[4 - \frac{2^{1/3}(1+\mathrm{i}3^{1/2})(5\nu_\varepsilon - 2)}{\beta(\nu_\varepsilon)} + \frac{2^{2/3}(1-\mathrm{i}3^{1/2})}{4(1-\nu_\varepsilon)}\beta(\nu_\varepsilon)\right], \qquad \text{(A.2c)}$$

where $\nu_\varepsilon \equiv (\nu + \varepsilon(1-\nu))/(1+2\varepsilon(1-\nu))$, $\mathrm{i} = (-1)^{1/2}$, and

$$\beta(\nu_\varepsilon) = \left[3^{3/2}\gamma(\nu_\varepsilon) + 56\nu_\varepsilon^3 - 123\nu_\varepsilon^2 + 78\nu_\varepsilon - 11\right]^{1/3}, \qquad \text{(A.3a)}$$

$$\gamma(\nu_\varepsilon) = \left[(1-\nu_\varepsilon)^3\left(32\nu_\varepsilon^3 - 16\nu_\varepsilon^2 + 21\nu_\varepsilon - 5\right)\right]^{1/2}. \qquad \text{(A.3b)}$$

Further, from the analysis of Lykotrafitis and Georgiadis [28], we notice that: (i) The zero $m_{1\varepsilon}$ is real for all values of ν_ε and coincides with the non-trivial zero of the Rayleigh function $R_\varepsilon(M_T, \varepsilon)$ in Eq. (12). (ii) The zeros $m_{2\varepsilon}$ and $m_{3\varepsilon}$ are also zeros of the function $(2-M_T^2)^2 + 4(1-M_{L\varepsilon}^2)^{1/2}(1-M_T^2)^{1/2}$. They are real in the interval $0 < \nu_\varepsilon \le \nu_0$, where $\nu_0 = 0.26308206488336365...$, and complex conjugate in the interval $\nu_0 < \nu_\varepsilon < 0.5$. We also notice that ν_0 is the real zero of $\gamma(\nu_\varepsilon)$. (iii) The inequalities $m_{1\varepsilon} < 1 < \mathrm{Re}\{m_{2\varepsilon}\} \le \mathrm{Re}\{m_{3\varepsilon}\}$ are valid. (iv) The inequalities $M_{L\varepsilon}^2 < M_T^2 \le m_\varepsilon^2 \le m_{2\varepsilon} < m_{3\varepsilon}$ are valid in the subsonic and transonic speed ranges, if, of course, $(m_{2\varepsilon}, m_{3\varepsilon})$ are real (i.e. for Poisson's ratios in the interval $0 < \nu_\varepsilon \le \nu_0$). (iv) The equality $m_{1\varepsilon}m_{2\varepsilon}m_{3\varepsilon} = 16(1-m_\varepsilon^{-2})$ is always valid.

In view of the above, the function $F_1^{(P)}\left(M_T,\varepsilon\right)$ in (11) can alternatively be written as

$$F_1^{(P)}\left(M_T,\varepsilon\right)=\frac{\left(1-M_{L\varepsilon}^2\right)^{1/2}\left[\left(2-M_T^2\right)^2+4\left(1-M_{L\varepsilon}^2\right)^{1/2}\left(1-M_T^2\right)^{1/2}\right]}{\pi\left(M_T^2-m_{1\varepsilon}\right)\left(M_T^2-m_{2\varepsilon}\right)\left(M_T^2-m_{3\varepsilon}\right)} \quad . \tag{A.4}$$

Then, passing to the limit in (A.4) as $V\to 0$, with the aid of the identity $m_{1\varepsilon}m_{2\varepsilon}m_{3\varepsilon}=16\left(1-m_\varepsilon^{-2}\right)$ and the pertinent expression for m_ε, one obtains that

$$F_1^{(P)}\left(0,\varepsilon\right)=-\frac{8}{\pi m_{1\varepsilon}m_{2\varepsilon}m_{3\varepsilon}}=-\frac{\left(1-\nu\right)\left(1+\varepsilon\right)}{\pi\left[1+2\varepsilon\left(1-\nu\right)\right]} \quad . \tag{A.5}$$

References

1. Craggs J.W., Roberts, A.M.: On the motion of a heavy cylinder over the surface of an elastic half-space. ASME J. Appl. Mech. **34**, 207-209 (1967)
2. Georgiadis, H.G., Barber, J.R.: On the super-Rayleigh / subseismic elastodynamic indentation problem, J. Elasticity **31**, 141-161 (1993)
3. Brock, L.M.: Some analytical results for heating due to irregular sliding contact of thermoelastic solids. Indian J. Pure Appl. Math. **27**, 1257-1278 (1996)
4. Brock, L.M.: Rapid sliding indentation with friction of a pre-stressed thermoelastic material. J. Elasticity **53**, 161-188 (1999)
5. Brock, L.M., Georgiadis, H.G.: Sliding contact with friction on a thermoelastic solid at subsonic, transonic and supersonic speeds. J. Thermal Stresses **23**, 629-656 (2000)
6. Brock, L.M, Georgiadis, H.G.: Multiple-zone sliding contact with friction on an anisotropic thermoelastic half-space. Int. J. Solids and Struct. **44**, 2820-2836 (2007)
7. Churilov, V.A.: Action of an elliptic stamp moving at a constant speed on an elastic half-space. J. Appl. Math. Mech. **42**, 1176-1182 (1978)
8. Rahman, M.: Hertz problem for a rigid punch moving across the surface of a semi-infinite elastic solid. ZAMM **47**, 601-615 (1996)
9. Gavrilov, S.N., Herman, G.C.: Oscillations of a punch moving on the free surface of an elastic half space. J. Elasticity **75**, 247-265 (2004)
10. Ju, F.D., Huang, J.H.: Heat checking in the contact zone of a bearing seal: A two-dimensional model of a single moving asperity. Wear **79**, 107-118 (1982)

11. Barber, J.R.: Thermoelastic displacements and stresses due to a heat source moving over the surface of a half plane. ASME J. Appl. Mech. **51**, 636-640 (1984)

12. Kennedy, F.D.: Thermal and thermomechanical effects in dry sliding. Wear **100**, 453-476 (1984)

13. Huang, J.H., Ju, F.D.: Thermomechanical cracking due to moving frictional loads. Wear **102**, 81-104 (1985)

14. Rosakis, A.J., Samudrala, O., Singh, R.P., Shukla, A.: Intersonic crack propagation in bimaterial systems. J. Mech. Phys. Solids **46**, 1789-1813 (1998)

15. Huang, Y., Wang, W., Liu, C., Rosakis, A.J.: Intersonic crack growth in bimaterial interfaces: An investigation of crack face contact. J. Mech. Phys. Solids **46**, 2233-2259 (1998)

16. Krylov V.V.: Generation of ground vibrations by superfast trains. Appl. Acoust. **44**, 149-164 (1995)

17. Lefeuve-Mesgouez, G., Lehouedec, D., Peplow, A.T.: Ground vibration in the vicinity of a high-speed moving harmonic strip load. J. Sound Vibration **231**, 1289-1309 (2000)

18. Ju, S.H.: Finite element analyses of wave propagations due to high-speed train across bridges. Int. J. Numer. Meth. Eng. **54**, 1391-1408 (2002)

19. Ju, S.H, Lin, H.T.: Analysis of train-induced vibrations and vibration reduction schemes above and below critical Rayleigh speeds by finite element method. Soil Dyn. Earthquake Eng. **24**, 993-1002 (2004)

20. Cole, J., Huth, J.: Stresses produced in a half plane by moving loads. ASME J. Appl. Mech. **25**, 433-436 (1958)

21. Georgiadis, H.G., Barber, J.R.: Steady-state transonic motion of a line load over an elastic half-space: The corrected Cole-Huth solution. ASME J. Appl. Mech. **60**, 772-774 (1993)

22. Barber, J.R.: Surface displacements due to a steadily moving point force. ASME J. Appl. Mech. **63**, 245-251 (1996)

23. Brock, L.M., Georgiadis, H.G.: Steady-state motion of a line mechanical / heat source over a half-space: A thermoelastodynamic solution. ASME J. Appl. Mech. **64**, 562–567 (1997)

24. Brock, L.M., Georgiadis, H.G.: Convection effects for rapidly moving mechanical sources on a half-space governed by fully coupled thermoelasticity. ASME J. Appl. Mech. **66**, 347-351 (1999)

25. Brock, L.M., Rodgers, M.J.: Steady-state response of a thermoelastic half-space to the rapid motion of surface thermal/mechanical loads. J. Elasticity **47**, 225-240 (1997)
26. Brock, L.M., Georgiadis, H.G., Tsamasphyros, G.: The coupled thermoelasticity problem of the transient motion of a line heat/mechanical source over a half-space. J. Thermal Stresses **20**, 773-795 (1997)
27. Georgiadis, H.G., Lykotrafitis G.: A method based on the Radon transform for three-dimensional elastodynamic problems of moving loads. J. Elasticity **65**, 87-129 (2001)
28. Lykotrafitis G., Georgiadis, H.G.: Three dimensional steady-state thermo-elastodynamic problem of moving sources over a half-space. Int. J. Solids and Struct. **40**, 899-940 (2003)
29. Biot, M.A.: Thermoelasticity and irreversible thermodynamics. J. Appl. Phys. **27**, 240-253 (1956)
30. Manolis, G.D., Beskos, D.E.: Integral formulation and fundamental solutions of dynamic poroelasticity and thermoelasticity. Acta Mech. **76**, 89-104 (1989)
31. Galin, L.A.: Contact problems in the theory of elasticity, (English translation from Russian by H. Moss), Sneddon, I.N., (Ed.), North Carolina State College, Department of Mathematics (1961)
32. Chadwick, P.: Thermoelasticity: The dynamical theory, In: Sneddon, I.N., Hill, R. (Eds.), Progress in Solid Mechanics. Vol. 1. North-Holland, Amsterdam, pp. 263-328 (1960)
33. Fung, Y.C.: Foundations of solid mechanics. Prentice-Hall, Englewood Cliffs, N.J. (1965)
34. Gelfand, I.M., Graev, M.I., Vilenkin, N.Ya.: In: Generalized functions, vol. 5. Academic Press, New York (1966)
35. Roos, B.W.: Analytic functions and distributions in physics and engineering. Wiley, New York (1969)
36. Lauwerier, H.A.: The Hilbert problem for generalized functions. Arch. Rat. Mech. Anal. **13**, 157-166 (1963)
37. Sokolnikoff, I.S.: Mathematical theory of elasticity. McGraw-Hill, New York (1956).
38. Rahman, M., Barber, J.R.: Exact expressions for the roots of the secular equation for Rayleigh waves. ASME J. Appl. Mech. **62**, 250-252 (1995)
39. Brock, L.M.: Analytic results for roots of two irrational functions in elastic wave propagtion. J. Austral. Math. Soc. Ser. B **40**, 72-79 (1998).
40. Walpole, L.J.: Some elastostatic and potential problems for an elliptic disc. Proc. Camb. Phil. Soc. **67**, 225-235 (1970)

41. Dyson, F.W.: The potentials of ellipsoids of variable densities. Quart. J. Math. Oxford ser. **XXV**, 259-288 (1891)
42. Gladwell, G.M.L.: Contact problems in the classical theory of elasticity. Sijthoff and Noordhoff, Alphen aan Rijn (1980)
43. Vorovich, I.I, Alexandrov, M., Babeshko, V.A.: Non-classical mixed boundary value problems of the theory of elasticity. Nauka. Moscow (1974) (in Russian)
44. Abramowitz, M., Stegun, I.A.: Handbook of mathematical functions. Dover, New York (1972)
45. Barber, J.R.: Elasticity. Kluwer Academic Publishers, Dordrecht (2002)